ELSEVIER

www.elsevier.nl/locate/jorganchem

Journal of Organometallic Chemistry 620 (2001) 32–38

Journal of Organometallic Chemistry

Synthesis and characterization of [Cp*Fe-dicyclopenta(a,f)naphthalene-FeCp*] and [Cp*Fe-dicyclopenta(a,f)naphthalene-FeCp*] BF$_4^-$

Geraldo Alfonso [a], Ivonne Chávez [a], Verónica Arancibia [a], Juan Manuel Manríquez [a,*], María Teresa Garland [b], Anna Roig [c], Elies Molins [c], Ricardo Fortunato Baggio [d]

[a] *Departamento de Química Inorgánica, Facultad de Química, Pontificia Universidad Católica de Chile, Casilla 306, Correo 22, Santiago, Chile*
[b] *Laboratorio de Cristalografía, Departamento de Física, Universidad de Chile, Chile.*
[c] *Institut de Ciéncia de Materials de Barcelona (CSIC), Campus UAB, 08193 Bellaterra, Barcelona, Spain*
[d] *Departamento de Física, Comisión Nacional de Energía Atómica, Buenos Aires, Argentina*

Received 7 April 2000; accepted 10 August 2000

Abstract

[Cp*Fe-dicyclopenta(a,f)naphthalene-FeCp*]$^{n+}$ (Cp* = pentamethylciclopentadiene, $n = 0$, 1), respectively named complexes **V** and **VI**, were synthesized and characterized. The X-ray structure has been solved and ^{1}H-, ^{13}C-NMR and elemental analysis were performed for the $n = 0$ complex. Cyclic voltammetry showed a potential difference of 360 mV within the two redox peaks. An absorption band at 850 nm was assigned to an intervalence band. The Mössbauer investigations show a uniform Fe^{2+} environment for the neutral compound and two sites, assigned to Fe^{2+} and Fe^{3+} for the monoxidized compound. The information gathered by all the previously mentioned techniques indicates that the studied binuclear compound belongs to the mixed valence class **II** using Robin and Day classification. © 2001 Elsevier Science B.V. All rights reserved.

Keywords: Iron complexes; Dihydrodicyclopentanaphthalene; Binuclear complexes; Mixed valence complexes

1. Introduction

The syntheses of bridged metallocene complexes derived from the $4n\pi$-electron hydrocarbon pentalene ($n = 2$) and its mono-benzologs, s- and as-indacene ($n = 3$), have received considerable attention, with special regard to the electronic interaction between metal centers [1–10].

It has been determined that the geometry of the bridging ligand plays an important role in the extent of delocalization of the mixed-valence derivatives for this family of compounds. Thus, for example, while ESR, Mössbauer, electrochemical and magnetic data for the diiron monocationic species [L(FeCp*)$_2$]$^+$ (L = pentalene, s-indacene), are consistent with a completely valence detrapped system, the analog monocationic as-indacene complex exhibits classical trapped ferrocene and ferrocenium centers [6].

In an effort to understand factors such as geometry of the bridging ligand and distance between the metal centers with the degree of delocalization in other members of this family, we have synthesized pentalene dibenzologs derivatives ($n = 4$).

The four members of the pentalene dibenzologs series as shown in Fig. 1 are: dicyclopenta(a,f)naphtalene (**I**), dicyclopenta(a,h)naphtalene (**II**), dicyclopenta(a,g) naphtalene (**III**) and the linearly annelated dicyclopenta(b,g)naphtalene (**IV**).

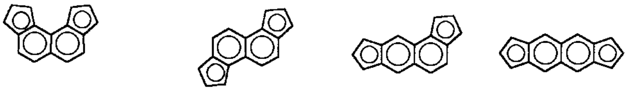

I **II** **III** **IV**

Fig. 1. **I** Dicyclopenta(a,h)naphthalene; **II** Dicyclopenta(a,f)naphthalene; **III** Dicyclopenta(a,g)naphthalene and **IV** Dicyclopenta(b,g)naphthalene

---

* Corresponding author. Tel.: + 56-2-6864397; fax: + 56-2-6864744.
E-mail address: galfonso@puc.cl (J.M. Manríquez).

PII: S0022-328X(00)00744-0

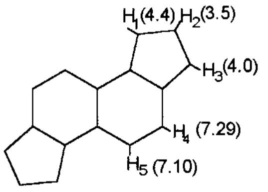

Fig. 2. Assignment of ^{1}H-NMR chemical shifts (δ) for **V**.

While none of the four members of this family are known in its neutral form, the dianions obtainable by the double deprotonation of the respective dihydrodicyclopenta-naphtalenes have been already described [4,11]. These bis(ligand)dimetal complexes of cobalt and iron of **II** were studied in preliminary reports. However, the characterization of the metal diiron species was complicated by their very low solubilities and the dicationic dicobalt derivative could only be obtained in a very low yield [4].

A previous work reported that the reaction of the dilithium salt of the bridging ligand with two equivalents of Cp*Fe(acac) (acac = acetylacetonate) provides a general route for the syntheses of linked ferrocenes [12]. Following this strategy, in this first paper, we reported the synthesis and structure of the biferrocene derivative of **1**, [Cp*Fe-dicyclopenta(a,f)nafphtalene-FeCp*] (**V**) and the study of the electronic delocalization of its mono-oxidized salt [Cp*Fe-dicyclopenta(a,f)nafphtalene-FeCp*]$^+$BF$_4^-$ (**VI**).

2. Results and discussion

*2.1. Synthesis and characterization of the complex [Cp*Fe-dicyclopenta(a, f)naphthalene-FeCp*] (V) and [Cp*Fe-dicyclopenta(a, f)nafphtalene-FeCp*]$^+$ BF$_4^-$ (VI)*

2.1.1. Synthesis of V

The preparation of the biferrocene **V**, has been previously reported [12,22,24]. Thus, reaction of the dilithium salt of **I** [11] with (η^5-C$_5$Me$_5$)Fe(acac), affords the title compound in about 45% yield along with a small amount of a material containing only one iron atom, probably **VII**, which were separated by column chromatography (Reaction (1)).

Compound **V** is obtained as air sensitive brown dark crystals from pentane. The ^{1}H-NMR spectrum of **V** shows a singlet at $\delta = 1.30$ (30H) assigned to the Cp* ring, a triplet at $\delta = 3.50$ (2H), two doublets at $\delta = 4.00$ (2H) and 4.40 (2H), and two doublets at $\delta = 7.10$ (2H) and 7.29 (2H). The peak assignments for the dicyclopentanapthalene ring are summarized in Fig. 2.

2.1.2. Synthesis of VI

Treatment of one equivalent of a THF solution of [Cp*Fe-dicyclopenta (a,f)nafphtalene-FeCp*] with one equivalent of ferrocenium tetrafluoroborate gives a dark precipitate of the salt [Cp*Fe-dicyclopenta-(a,f)nafphtalene-FeCp*]$^+$BF$_4^-$ (**VI**). Blue crystals of **VI** were obtained after recrystallization of the solid by a slow diffusion of the diethyl ether into a concentrated dicloromethane (DCM) solution of the salt. The crystals were found to be air-sensitive.

*2.2. X-ray structural determination of [Cp*Fe-dicyclopenta(a, f)naphthalene-FeCp*] (V)*

The structure resolution of **V** by X-ray single crystal diffraction shows the two fragments of Cp*Fe in *trans* position, displaying a η^5 type bond to the bridging ligand. The molecule is planar without large distortions (maximum deviations from mean plane: 0.06 Å for the outermost carbons C(26) and C(33)).

Bonds distances and angles have similar values to those found in related systems (see Fig. 3 and Tables 1 and 2). The planar Cp* and Cp* groups sharing a common iron atom are almost parallel to each other, with angles between normal of 3.5 and 3.1° at the Fe(1) and Fe(2) ends, respectively. They present one of the major differences found in the otherwise almost centrosymmetric molecule, as it is the relative rotation between parallel pentagonal groups along an axis through their centers, the first pair is almost eclipsed, with a relative rotation of ca. 6.6°, while the second presents a much larger misfit of more than 27°.

Both Cp* groups interact in a similar way to their respective Fe atoms (Cp*–Fe(1), 1.632(3) Å; Cp*–Fe(2), 1.642(4) Å; carbon(Cp*)–Fe(1), 2.02–2.03 Å; carbon(Cp*)–Fe(2), 2.02–2.05 Å. These latter C–Fe ranges result in a situation where the projection of the iron atom into the Cp* plane is almost coincident with

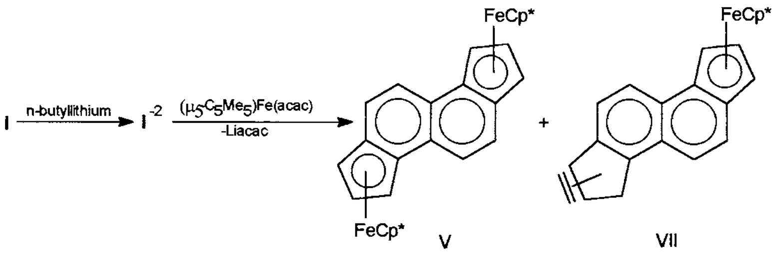

(1)

the pentagon center itself, with an almost zero drift between them (‘slippage’). This is an expected fact and agrees with previously published results [6]. Similar considerations of resemblance can be made about both Cp groups of the organic ligand; Cp–Fe(1), 1.668(4) Å; Cp–Fe(2), 1.667(4) Å; carbon(Cp)–Fe(1), 2.00–2.13 Å; carbon(Cp)–Fe(2), 2.02–2.11 Å. These broader ranges, in turn, are evident of a net iron ‘slippage’ of ca. 0.1 Å towards the mid-point of one of the outermost C–C bonds in the Cp (C(26)–C(27)) in the case of Fe(1), and C(34)–C(35) and the case of Fe(2).

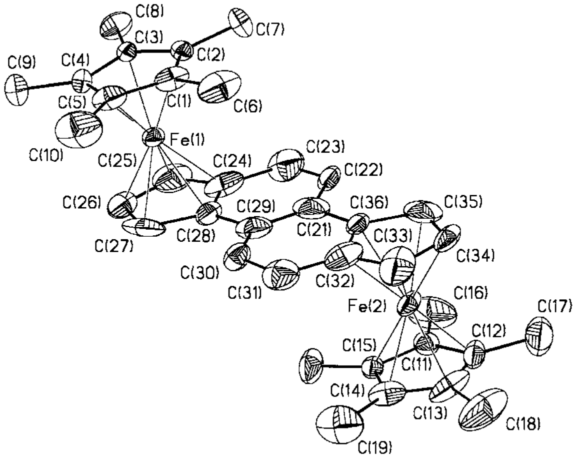

Fig. 3. Crystal structure diagram of [Cp*Fe-dicyclopenta-(a,f)naphthalene-FeCp*]. Displacement ellipsoids drawn at 40% level. Hydrogen atoms not shown, for the sake of simplicity.

Table 1
Crystal data and structure refinement of complex **V**

Identification code	*trans*-Cp*–Fe
Empirical formula	$C_{36}H_{40}Fe_2$
Formula weight	584.38
Temperature (K)	293(2)
Wavelength (Å)	0.71073
Crystal system	Orthorhombic
Space group	*Pbca*
Unit cell dimensions	
a (Å)	16.41(2)
b (Å)	17.473(13)
c (Å)	20.00(2)
α (°)	90
β (°)	90
γ (°)	90
V (Å^3)	5737(8)
Z	8
D_{calc} (Mg/m^3)	1.353
Absorption coefficient (mm^{-1})	1.035
F(000)	2464
Crystal size (mm)	$0.32\times0.28\times0.24$
Theta range for data collection (°)	1.98–25.02
Limiting indices	$0<h<14$, $0<k<20$, $0<l<23$
Reflections collected	4722
Independent reflections	4554 [$R_{int}=0.068$]
Absorption correction	Psi_scan
Max/min transmission	0.75, 0.71
Refinement method	Full-matrix least-squares on F^2
Data/restraints/parameters	4554/107/353
Goodness-of-fit on F^2	1.022
Final R indices [$I>2\sigma(I)$]	$R_1=0.0570$, $wR_2=0.1322$
R indices (all data)	$R_1=0.0943$, $wR_2=0.1508$
Largest difference peak and hole (e A^{-3})	0.888 and -0.533

Table 2
Fractional atomic coordinates ($\times10^4$) and equivalent isotropic displacement parameters (Å$^2\times10^3$) of complex **V**

Fe(1)	7745(1)	2030(1)	4982(1)	33(1)
Fe(2)	5505(1)	364(1)	7543(1)	45(1)
C(1)	6720(3)	2589(3)	4708(3)	46(2)
C(2)	7287(4)	3112(3)	4965(3)	34(1)
C(3)	8004(3)	3065(3)	4571(2)	29(1)
C(4)	7864(4)	2507(3)	4063(2)	37(1)
C(5)	7070(4)	2210(3)	4147(3)	51(2)
C(6)	5866(4)	2462(5)	4980(4)	86(2)
C(7)	7159(5)	3639(4)	5545(3)	73(2)
C(8)	8767(4)	3533(3)	4649(3)	52(2)
C(9)	8460(5)	2299(4)	3524(3)	83(3)
C(10)	6665(6)	1617(5)	3724(5)	105(3)
C(11)	6458(4)	141(3)	8177(3)	40(1)
C(12)	5693(5)	2(4)	8490(3)	65(2)
C(13)	5278(4)	−569(5)	8113(4)	73(3)
C(14)	5774(4)	−768(3)	7578(3)	52(2)
C(15)	6500(3)	−334(3)	7613(2)	32(1)
C(16)	7112(6)	683(4)	8412(5)	100(3)
C(17)	5392(6)	386(5)	9102(4)	109(3)
C(18)	4453(6)	−922(6)	8256(5)	128(4)
C(19)	5604(6)	−1349(5)	7032(4)	103(3)
C(20)	7216(4)	−378(4)	7145(3)	72(2)
C(21)	6451(4)	1411(3)	6533(3)	73(2)
C(22)	6973(4)	1964(3)	6861(2)	49(2)
C(23)	7726(5)	2145(4)	6591(3)	80(3)
C(24)	7989(4)	1742(4)	5998(3)	70(2)
C(25)	8708(4)	1800(4)	5628(3)	75(2)
C(26)	8671(4)	1278(3)	5089(3)	55(2)
C(27)	7878(4)	900(3)	5114(3)	76(3)
C(28)	7489(3)	1215(3)	5707(3)	43(2)
C(29)	6691(4)	1020(3)	5986(3)	66(2)
C(30)	6163(4)	484(3)	5666(3)	46(2)
C(31)	5434(4)	254(4)	5959(3)	75(2)
C(32)	5175(4)	650(4)	6556(3)	69(2)
C(33)	4479(5)	556(5)	6955(4)	92(3)
C(34)	4533(4)	1082(4)	7496(3)	63(2)
C(35)	5295(5)	1496(4)	7435(3)	87(3)
C(36)	5664(3)	1202(3)	6828(2)	38(1)

2.3. Electrochemical characterization of [Cp*Fe-dicyclopenta(a, f)naphthalene-FeCp*]

Cyclic voltammetry studies of **V** were carried out in DCM. The cyclic voltamogramms present two quasi-reversible redox processes with similar peak heights and similar peak current ratios (see Fig. 4). The values of the potential changes slightly with the scan rates. At 0.05 V s^{-1} the oxidation occurs at 0.15 and 0.51 V versus SCE (peaks **a** and **b**) and the products generated on the electrode surface are reduced at 0.31 and −0.06 V versus SCE (peaks **c** and **d**). Controlled potential electrolysis at 0.35 V versus SCE ($E_{\mathrm{peak}} = 0.15$ V) allowed us to determine that one equivalent of charge per mol of complex has been transferred in this process.

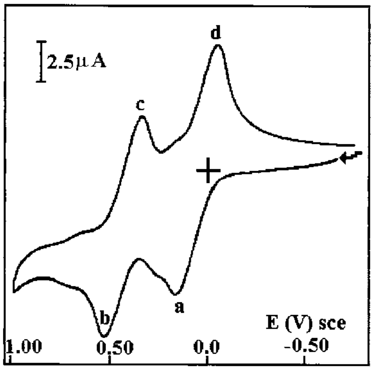

Fig. 4. Cyclic voltammogram of [Cp*Fe-dicyclopenta-(a,f)naphthalene-FeCp*] complex 3.0 mM in CH_2Cl_2 (0.1 M Tetrabutylammonium tetrafluoroborate, TBATFB; scan rate 0.05 V s^{-1}).

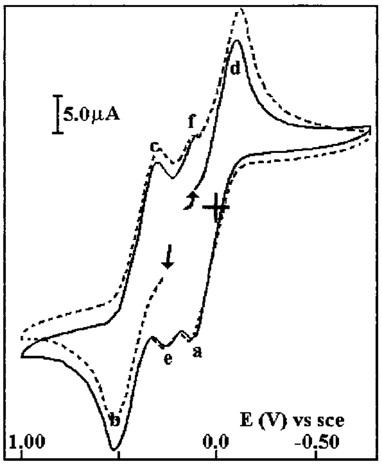

Fig. 5. (a) and (b) Cyclic voltammogram of [Cp*Fe-dicyclopenta-(a,f)naphthalene-FeCp*]$^+$$BF_4^-$ complex 3.0 mM in CH_2Cl_2 0.1 M Tetrabutylammonium tetrafluoroborate, TBATFB; scan rate 0.05 V s^{-1}.

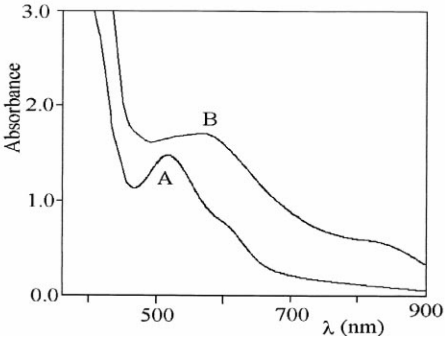

Fig. 6. (A) Electronic Absorption Spectra of [Cp*Fe-dicyclopenta-(a,f)naphthalene-FeCp*] complex 3.0 mM in CH_2Cl_2. (B) Electronic Absorption Spectra of [Cp*Fe-dicyclopenta(a,f)naphthalene-FeCp*]$^+$ BF_4^- complex 3.0 mM in CH_2Cl_2.

The initial dark red solution changes to a violet color solution. Back electrolysis re-established the original binuclear complex. After a second electrolysis at 0.71 V versus SCE ($E_{\mathrm{peak}} = 0.51$ V), *trans*-[Cp*Fe-dicyclopenta(a,f)naphthalene-FeCp*] is completely oxidized, in this case the color of the solution becomes brown.

The difference of potential between the oxidation peaks is 0.36 V ($\Delta E = 360$ mV) such as the difference between the $\Delta E_{1/2}$. This value of ΔE, indicates moderate electronic interaction between the iron atoms, characteristic of a class **II** compound following Robin and Day's classification [13–15]. On the other hand, both oxidized complexes are stable in a solution of DCM without oxygen. The mixed valence complex, peak current ratio is equal to unit ($I_{\mathrm{pa}}/I_{\mathrm{pc}} = 1$) while with the completely oxidized complex, the peak current ratio is slightly deviated of unity (see Fig. 5(a) and (b)).

Two small shoulders are observed in both figures at 0.26 and 0.11 V versus SCE (peaks **e** and **f**), which would indicate that a small reaction occurs at the electrode surface and it is not possible to characterize it.

A UV–Vis-NIR spectrum was recorded for the complex **V** (see Fig. 6(A)). The mixed-valence complex obtained for electrolysis in DCM presents an 'intervalence-transfer' band at 850 nm. This band is not present in the neutral complex and is not observed when *trans*-[Cp*Fe-dicyclopenta(a,f)naphthalene-FeCp*] is oxidized twice [16–18]. The same band is observed for *trans*-[Cp*Fe - dicyclopenta(a,f)naphthalene - FeCp*]$^+$$BF_4^-$ prepared by chemical procedures (see Fig. 6(B)). The position of the 'intervalence-transfer' of complex **VI**, when recorded in acetonitrile and acetone shifts to 812 and 800 nm, respectively. The solvent dependence of this band is also a characteristic feature of complexes that belong to class **II**.

2.4. Mössbauer spectroscopy characterization of V and VI

Mössbauer spectroscopy is a local probe method. It is very sensitive to the iron electronic oxidation state and to its crystallographic environment.

Mössbauer spectra were collected at 90 K. Table 3 shows the Mössbauer hyperfine parameters for the neutral compound [Cp*Fe-dicyclopenta(a,f)naphthalene-FeCp*] and for the mixed-valence salt [Cp*Fe-dicyclopenta(a,f)naphthalene-FeCp*]$^+$$BF_4^-$. Fig. 7(a) and (b) shows the Mössbauer spectra of the two compounds.

The spectrum of the neutral compound [Cp*Fe-dicyclopenta(a,f)naphthalene-FeCp*] shows an unique Fe^{2+} site. The mixed-valence salt of [Cp*Fe-dicyclopenta(a,f) naphthalene-FeCp*]$^+$$BF_4^-$ shows iron in two oxidation states (Fe^{2+} and Fe^{3+}) with areas close to 50% assigned to each sub-spectrum [19,20]. This result

Table 3
Hyperfine parameters for the fitting of the Mössbauer spectra [a]

Sample	Site	δ_{Fe} (mms^{-1})	ΔEq (mms^{-1})	Γ (mms^{-1})	Area (%)	χ^2
[Cp*Fe-dicyclopenta(a,f)naphthalene-FeCp*]	Fe^{2+}	0.527(1)	2.38(1)	0.26(1)	100	1.0
[Cp*Fe-dicyclopenta(a,f)naphthalene-FeCp*]-BF_4	Fe^{2+} Fe^{3+}	0.525(1) 0.525(1)	2.39(1) 0.63(1)	0.24(1) 0.26(1)	44(5) 56(5)	1.0

[a] δ_{Fe}, ΔEq and Γ are the isomer shift, quadrupole splitting and the full width at half maximum, respectively. The Area represents the Mössbauer fraction of each sub-spectrum in relative percentage. The χ^2 parameter is also given. The errors are given within brackets and correspond to the last digit.

coupled with cyclic voltammetry and the solvent dependence of the intervalence-transfer band indicates that the mixed-valence compound has a localized charge density and could be a class **II** compound following Robin and Day's classification [21].

3. Experimental

3.1. General

Using standard Schlenck techniques under a nitrogen atmosphere, all manipulations were carried out involving air-sensitive materials. $Fe(acac)_2$ [22], $[Cp_2Fe]^+BF_4^-$ [23] and dihydrodicyclopenta(a,f)naphthalene [4,11] were prepared according to published procedures. 2,6 dimethylnaphthalene was from Aldrich. THF, diethyl ether, pentane and toluene were distilled from sodium benzophenone ketyl.

IR spectra were recorded on a Perkin–Elmer 1710 FT spectrophotometer using a Nujol mull. Elemental analyses were made with a Fison 1108 microanalyser.

NMR analysis was performed with a Bruker/200P, ^{1}H (200 MHz) and ^{13}C (50 MHz) spectrometer with TMS as reference.

3.1.1. X-ray crystallography

3.1.1.1. Crystal data. $C_{36}H_{40}Fe_2$; $M = 584.38$, orthorhombic, space group *Pbca*, $a = 16.41(2)$, $b = 17.473(13)$, $c = 20.00(2)$ Å, $V = 5737(8)$ Å^3, $Z = 8$, $D_{\mathrm{calc}} = 1.353$ g cm^{-3}, $F(000) = 2464$, $\lambda(\text{Mo–K}_\alpha) = 0.71073$ Å, $\mu = 1.035$ mm^{-1}, $T = 180$ K.

3.1.1.2. Data collection and structure refinement. Data for X-ray structure determination were gathered with a single crystal Siemens R3m diffractometer, using graphite monocromatized Mo–K$_\alpha$ radiation. The redish crystals were obtained from diffusion of diethyl ether into a DCM solution.

The process of structure resolution was cumbersome, impaired by the fact that the X-ray beam damashed specimens suitable for crystal structure analysis, even when encapsulated in an inert atmosphere. Data were collected near 180 K to minimize deterioration. The final specimen used was a polyhedron measuring $0.32 \times 0.28 \times 0.24$ mm^3. Cell parameters were obtained by least squared refinement of 25 reflections in the range $15 \leq 2\theta \leq 30°$. A total of 4554 unique reflections were collected, and corrected for absorption effects by a semiempirical method (psi-scan, $\mu = 1.035$ mm^{-1}, $T_{\max} = 0.75$, $T_{\min} = 0.71$).

The structure was solved by direct methods (SHELXS 97, 25a and refined by full matrix least squares in F^2 (SHELXL 97 25b down to a final discrepancy factor $R = 0.057$. To achieve these, similar restraints had to be applied to homologous distances to the organic ligands at the early stages of refinement. These ligands were relaxed at the final stages of the procedure. Hydrogen atoms were positioned at their expected values, with both coordinates and temperature factors riding onto their host atoms. Final atomic positions are presented in Tables 1 and 2 and selected geometric parameters are presented in table Table 4. There are no unusual contacts in the packing, which is controlled by typical Van der Waals interactions.

3.1.2. Cyclic voltammetry of V

Cyclic voltammetry measurements were carried out with a Bank potentiostat (model Wenking ST-72) coupled to a voltage scan generator (model USG-72) and a

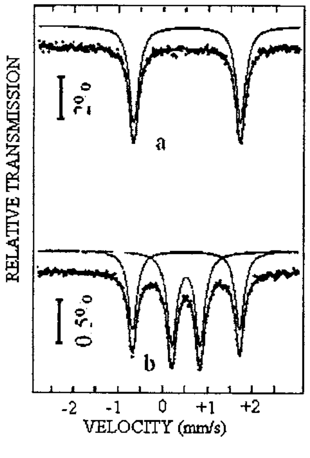

Fig. 7. (a) Mössbauer Spectrum of [Cp*Fe-dicyclopenta(a,f)naphthalene-FeCp*]. (b) Mössbauer Spectrum of $[\text{Cp*Fe-dicyclopenta(a,f)naphthalene-FeCp*}]^+BF_4^-$.

Table 4
Bond distances (Å) of complex **V**

Fe(1)–C(27)	2.004(6)	C(4)–C(9)	1.500(8)
Fe(1)–C(26)	2.020(6)	C(5)–C(10)	1.494(9)
Fe(1)–C(1)	2.022(6)	C(11)–C(15)	1.403(7)
Fe(1)–C(4)	2.028(5)	C(11)–C(12)	1.423(9)
Fe(1)–C(5)	2.029(6)	C(11)–C(16)	1.507(9)
Fe(1)–C(3)	2.031(5)	C(12)–C(13)	1.425(11)
Fe(1)–C(2)	2.034(5)	C(12)–C(17)	1.481(9)
Fe(1)–C(28)	2.076(5)	C(13)–C(14)	1.389(10)
Fe(1)–C(25)	2.079(7)	C(13)–C(18)	1.515(11)
Fe(1)–C(24)	2.131(6)	C(14)–C(15)	1.414(8)
Fe(1)–Cp*	1.632(3)	C(14)–C(19)	1.517(9)
Fe(1)–Cp	1.668(4)	C(15)–C(20)	1.504(8)
Fe(2)–C(35)	2.019(6)	C(21)–C(29)	1.349(8)
Fe(2)–C(12)	2.021(6)	C(21)–C(22)	1.449(6)
Fe(2)–C(13)	2.024(6)	C(21)–C(36)	1.465(7)
Fe(2)–C(14)	2.028(6)	C(22)–C(23)	1.385(7)
Fe(2)–C(34)	2.032(6)	C(23)–C(24)	1.445(7)
Fe(2)–C(15)	2.044(5)	C(24)–C(28)	1.364(7)
Fe(2)–C(11)	2.052(6)	C(24)–C(25)	1.397(7)
Fe(2)–C(36)	2.063(5)	C(25)–C(26)	1.414(7)
Fe(2)–C(33)	2.081(7)	C(26)–C(27)	1.461(7)
Fe(2)–C(32)	2.106(6)	C(27)–C(28)	1.455(6)
Fe(2)–Cp*	1.642(4)	C(28)–C(29)	1.463(7)
Fe(2)–Cp	1.667(4)	C(29)–C(30)	1.427(6)
C(1)–C(2)	1.402(8)	C(30)–C(31)	1.391(7)
C(1)–C(5)	1.424(9)	C(31)–C(32)	1.445(7)
C(1)–C(6)	1.519(9)	C(32)–C(36)	1.367(7)
C(2)–C(3)	1.419(7)	C(32)–C(33)	1.403(7)
C(2)–C(7)	1.496(7)	C(33)–C(34)	1.424(7)
C(3)–C(4)	1.427(7)	C(34)–C(35)	1.449(7)
C(3)–C(8)	1.504(8)	C(35)–C(36)	1.452(6)
C(4)–C(5)	1.413(8)		

Graphtec recorder (model WX-1100). The auxiliary electrode was a platinum-coil electrode, which was isolated from the bulk solution by a glass tube with a porosity glass frit at the end; it contained a 0.2 M solution of supporting electrolyte. The reference was a Ag | AgCl electrode (aqueous tetramethylammonium chloride), cracked galls bead electrode, which was adjusted to 0.00 V with the saturated calomel electrode (SCE). The reference electrode was located inside a Luggin capillary in the cell compartment. All the experiments were performed under argon atmosphere, at room temperature (r.t.) (20°C) in CH_2Cl_2 solution. Solutions were 2 mM in complex and 200 mM in tetraethylammonium perchlorate (TEAP) as supporting electrolyte.

3.1.3. Mössbauer spectroscopy of ***V*** *and* ***VI***

The Mössbauer spectra were obtained using a constant acceleration Mössbauer spectrometer with a ^{57}Co–Rh source. The source was moved via triangular velocity waveform and the γ-counts were collected in a 512 multi-channel analyzer.

Velocity calibration was done using a 25 µm thick metallic Fe foil, and the Mössbauer spectral parameters are given relative to this standard at r.t. The spectra were taken with the sample placed in a chamber under an inert nitrogen atmosphere to avoid any further oxidation.

*3.2. Synthesis of [Cp*Fe-dicyclopenta(a, f)naphthalene-FeCp*] (V)*

A solution of $Fe(acac)_2$ (1.22 g, 4.80 mmol) dissolved in THF (30 ml) was cooled to −78°C and a suspension of Cp*Li (0.68 g, 4.80 mmol) in THF (25 ml) was added. The mixture was warmed to r.t. A hexane solution of *n*-butyllithium (1.6 M, 3 ml, 4.80 mmol) was added dropwise to dihydrodicyclopenta(a,f)naphthalene (0.49 g, 2.40 mmol) dissolved in THF (20 ml) at −78°C. Dilithium dicyclopenta(a,f)naphthalene was formed. The mixture was warmed to r.t. The Cp*Fe(acac) solution was added with stirring to the dilithium dicyclopenta(a,f)naphthalene at −78°C. The mixture was warmed to r.t. and stirred for 2 h. Solvent was removed in vacuo and the product was extracted several times with toluene until the extractions became colorless. The combined extracts were put together and the solvent evaporated to dryness. The crude product was chromatographed on neutral aluminum oxide (25.0 g, 150 mesh, standard grade) eluting with pentane, yielding 0.63 g (1.08 mmol, 45%) of brown dark crystals. Elemental analysis for $C_{36}H_{40}Fe_2$: Anal. Calc.: C, 73.97; H, 6.85. Found: C, 73.05; H, 6.76%.

^{1}H-NMR (C_6D_6) δ ppm: δ *CCH* 7.29 (d, 2H), δ *CCCH* 7.10 (d, 2H), δ *CCCH* 4.40 (dd, 2H), δ *CCH* 4.00 (dd, 2H), δ *CHCHCH* 3.50 (t, 2H) and δ CH_3 1.30 (s, 30H).

^{13}C-NMR: (C_6D_6) δ ppm: 127,14; 123,15; 87,38; 79,77; 79,46; 79,14; 75,76; 68,06; 65,53; 12,18.

*3.3. Synthesis of [Cp*Fe-dicyclopenta(a, f)naphthalene-FeCp*] BF_4 (VI)*

Cp*Fe-dicyclopenta(a,f)naphthalene-FeCp* (150 mg, 0.26 mmol) dissolved in 20 ml of THF was added to $[FeCp_2]^+[BF_4]^-$ (70 mg, 0.26 mmol) and the mixture was stirred at r.t. for 4 h resulting in the formation of a blue precipitate. The mixture was filtered and the insoluble material was washed with diethyl ether to remove all the ferrocene and dried in vacuo. The solid was recrystallized by slow diffusion of diethyl ether into a concentrated DCM solution of **VI**. Blue crystals were observed within 24 h. The crystals were filtered, washed with diethyl ether, and dried in vacuo, the yield of **VI** was 0.13 g. (0.19 mmol, 75%). Elemental analysis for $C_{36}H_{40}Fe_2BF_4$: Anal. Calc.: C, 64.44; H, 5.97. Found: C, 64.32; H, 5.86%.

4. Conclusions

From our results we can conclude that [Cp*Fe-dicyclopenta(a,f)naphthalene-FeCp*] BF_4 (**VI**) complex is the tipic, a compound of the mixed valence type, with moderate interaction between the metallic centers. This was evaluated for the different techniques applied for this study and characterization of this salt.

5. Supplementary material

Full details of the atomic parameter and bond lengths and angles have been deposited with the Cambridge Crystallographic Date Centre, CCDC nos. 142591 and 142592 for *cis*-Cp*Fe(acac) and *trans*-Cp*Fe-dicyclopenta(a,f)naphthalene-FeCp*, respectively. Copies of this information may be obtained free of charge from The Director, CCDC, 12 Union Road, Cambridge CB2 1EZ, UK (fax: +44-1223-336033; e-mail: deposit@ccdc.cam.ac.uk or http://www.ccdc.cam.ac.uk)

Acknowledgements

We thank the CEE,CI1-CT91-0913 proyect, Cátedra Presidencial en Ciencias 1996 (J.M. Manríquez), Fondecyt No. 8 980 007, Fondecyt No. 2 990 005 (G. Alfonso) and Fundación Andes for proyect 'Apoyo a la Física Experimental' (M.T. Garland) for financial support. We are very grateful to Dr Beatriz Oelckers, Lic Nadime Daire and MSc Giovani Visconti for their participation in the synthesis of the ligand.

References

[1] S. Barlow, D. O'Hare, Chem. Rev. 97 (1997) 637.
[2] T.J. Katz, J. Schulman, J. Am. Chem. Soc. 86 (1964) 3169.
[3] T.J. Katz, N Acton, J. McGinnis, J. Am. Chem. Soc. 94 (1972) 6205.
[4] T.J. Katz, W. Sluzarek, J. Am. Chem. Soc. 101 (1978) 4259.
[5] W.L. Bell, C.J. Curtis, C.W. Eigenbrot, C.G. Pierpont, J.L. Robbins, J.C. Smart, Organometallics 6 (1978) 266.
[6] J.M. Manríquez, M.D. Ward, W. Reiff, J.C. Calabrese, N.L. Jones, P.J. Carrol, E.E. Bunel, J.S. Miller, J. Am. Chem. Soc. 117 (1995) 6182.
[7] S. Barlow, D. O'Hare, Organometallics 15 (1996) 3483.
[8] S. Barlow, D.R. Cary, M.J. Drewitt, D. O'Hare, J. Chem. Soc. Dalton Trans. (1997) 3867.
[9] D.R. Cary, J.C. Gren, D. O'Hare, Angew. Chem. Int. De. Engl. 36 (1997) 2618.
[10] D.R. Cary, C.G. Webster, M.J. Drewitt, S. Barlow, J.C. Gren, D. O'Hare, Chem. Commun. (1997).
[11] R.S. Schneider, E.T. Ullman, Tetrahedron Lett. 38 (1969) 3249.
[12] E.E. Bunel, P. Campos, J. Ruiz, L. Valle, I. Chadwick, M. Santa Ana, G. Gonzalez, J.M. Manriquez, Organometallics 7 (1988) 474.
[13] V. Kolle, J. Grub, J. Organomet. Chem. 133 (1985) 133.
[14] M.D. Ward, in: A.J. Bard (Ed.), Electroanalytical Chemistry, Marcel Dekker, New York, 1989, p. 181.
[15] D. Osella, L. Milone, C. Nervi, M. Ravera, J. Organomet. Chem. 488 (1995) 1.
[16] O.V. Gusev, S. Sergeev, I.M. Saez, P.M. Maitlis, Organometallics 13 (1994) 2059.
[17] D.L. Reger, S.A. Klaeren, J.E. Babin, R.D. Adams, Organometallics 7 (1988) 181.
[18] P. Diversi, S. Lacoponi, G. Ingroso, A. Laschi, P. Zanello, J. Chem. Soc. Dalton Trans. (1993) 351.
[19] D.N. Hendrickson, M.J. Cohn, M.D. Timken, J. Am. Chem. Soc. 106 (1984) 6683.
[20] S.L. Lee, S.J. Li, T.Y. Dong, C.C. Schei, T.L. Hsu, Inorg. Chem. 30 (1991) 2475.
[21] (a) M.B. Robin, P. Day, Advan. Inorg. Radiochem. 10 (1967) 247. (b) G.C. Allen, N.S. Hush, Progress Inorg. Chem. 8 (1967) 357.
[22] (a) E.E. Bunel, J.M. Manríquez, L. Valle, Organometallics 4 (1985) 1680. (b) J.M. Manríquez, E.E. Bunel, B. Oelckers, Inorg. Synth. 31 (1997) 214.
[23] Y. Einaga, Y. Yamada, T. Tominaga, J. Radional. Nucl. Chem. 218 (1997) 97.
[24] An alternative procedure to Cp*Fe(acac) has recently appeared see G.E. Herberich, A. Gaffke, H.J. Eckenrath, Organometallics 17 (1998) 5931.
[25] (a) G.M. Sheldrick, SHELXS 97, Program for the solution of Structure Resolution, University of Gottingen, Gottingen, Germany, 1997. (b) G.M. Sheldrick, SHELXL 97, Program for the solution of Structure Refinement, University of Gottingen, Gottingen, Germany, 1997.